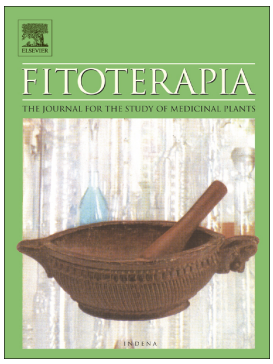

Bufadienolides and anti-angiogenic homoisoflavonoids from Rhodocodon cryptopodus, Rhodocodon rotundus and Rhodocodon cyathiformis

Hannah Whitmore, Kamakshi Sishtla, Walter Knirsch, Jacky L. Andriantiana, Sianne Schwikkard, Eduard Mas-Claret, Sarah M. Nassief, Sani M. Isyaka, Timothy W. Corson, Dulcie A. Mulholland

PII: S0367-326X(19)32327-5

DOI: https://doi.org/10.1016/j.fitote.2020.104479

Reference: FITOTE 104479

To appear in: *Fitoterapia*

Received date: 6 December 2019

Revised date: 7 January 2020

Accepted date: 8 January 2020

Please cite this article as: H. Whitmore, K. Sishtla, W. Knirsch, et al., Bufadienolides and anti-angiogenic homoisoflavonoids from Rhodocodon cryptopodus, Rhodocodon rotundus and Rhodocodon cyathiformis, *Fitoterapia* (2020), https://doi.org/10.1016/j.fitote.2020.104479

Bufadienolides and Anti-angiogenic homoisoflavonoids from *Rhodocodon cryptopodus, Rhodocodon rotundus* and *Rhodocodon cyathiformis*.

Hannah Whitmore [a], Kamakshi Sishtla [b], Walter Knirsch [c], Jacky L. Andriantiana [d], Sianne Schwikkard [e], Eduard Mas-Claret [a], Sarah M. Nassief [a], Sani M. Isyaka [a,f], Timothy W. Corson [b*], Dulcie A. Mulholland [a,f, **]

[a] *Natural Products Research Group, Department of Chemistry, University of Surrey, Guildford, GU2 7XH; United Kingdom*

[b] *Eugene and Marilyn Glick Eye Institute, Department of Ophthalmology, Indiana University School of Medicine, 1160 W. Michigan St., Indianapolis, IN 46202, U.S.A.*

[c] *Institute of Plant Sciences, NAWI Graz, Karl-Franzens University Graz, Holteigasse 6, A-8010, Graz, Austria*

[d] *Parc Botanique et Zoologique de Tsimbazaza, Rue Fernand Kassanga, Antananarivo 101, Madagascar*

[e] *School of Life Sciences, Pharmacy and Chemistry, Kingston University, Kingston-upon-Thames, KT1 2EE, United Kingdom*

[f] *School of Chemistry and Physics, University of Kwazulu-Natal, Durban, South Africa*

Abbreviations: AMD, age-related macular degeneration; CD, circular dichroism; COSY, correlation spectroscopy; EBM, endothelial basal medium; EGM, endothelial growth medium; FBS, foetal bovine serum; FTIR, Fourier-transform infrared; HMBC, heteronuclear multiple bond spectroscopy; HRECs, human retinal microvascular endothelial cells; HRESIMS, high- resolution electrospray ionization mass spectrometry; LC-MS, liquid chromatography-mass spectrometry; NMR, nuclear magnetic resonance; NOESY, Nuclear Overhauser effect spectroscopy; PDR, proliferative diabetic retinopathy; ROP, retinopathy of prematurity; TOF, time of flight; VEGF, vascular endothelial growth factor.

*Corresponding Author. Eugene and Marilyn Glick Eye Institute, Department of Ophthalmology, Indiana University School of Medicine, 1160 W. Michigan St., Indianapolis, IN 46202, U.S.A. E-mail address: tcorson@iu.edu

**Corresponding Author. Natural Products Research Group, Department of Chemistry, Faculty of Engineering and Physical Sciences, University of Surrey, Guildford GU2 7XH, United Kingdom. E-mail address: d.mulholland@surrey.ac.uk

ABSTRACT

Background: Homoisoflavonoids have been shown to have potent anti-proliferative activities in endothelial cells over other cell types and have demonstrated a strong antiangiogenic potential in vitro and in vivo in animal models of ocular neovascularization. Three species of *Rhodocodon* (Scilloideaea subfamily of the Asparagaceae family), endemic to Madagascar, *R. cryptopodus*, *R. rotundus* and *R. cyathiformis*, were investigated.

Purpose: To isolate and test homoisoflavonoids for their antiangiogenic activity against human retinal microvascular endothelial cells (HRECs), as well as specificity against other ocular cell lines.

Methods: Plant material was extracted at room temperature with EtOH. Compounds were isolated using flash column chromatography and were identified using NMR and CD spectroscopy and HRESIMS. Compounds were tested for antiproliferative effects on primary human microvascular retinal endothelial cells (HRECs), ARPE19 retinal pigment epithelial cells, 92-1 uveal melanoma cells, and Y79 retinoblastoma cells. HRECs exposed to compounds were also tested for migration and tube formation ability.

Results: Two homoisoflavonoids, 3*S*-5,7-dihydroxy-(3'-hydroxy-4'-methoxybenzyl)-4-chromanone (**1**) and 3*S*-5,7-dihydroxy-(4'-hydroxy-3'-methoxybenzyl)-4-chromanone (**2**), were isolated along with four bufadienolides. Compound **1** was found to be non-specifically antiproliferative, with GI_{50} values ranging from 0.21 – 0.85 µM across the four cell types, while compound **2** showed at least 100-fold specificity for HRECs over the other tested cell lines. Compound **1**, with a 3*S* configuration, was 700 times more potent that the corresponding 3*R* enantiomer recently isolated from a *Massonia* species.

Conclusion: Select homoisoflavonoids have promise as antiangiogenic agents that are not generally cytotoxic.

Keywords:

Rhodocodon

Homoisoflavonoids

Bufadienolides

Anti-angiogenic

Neovascularization

Endothelial cells

Introduction

Abnormal formation of new blood vessels in the eye is associated with blindness in many ocular diseases such as retinopathy of prematurity (ROP) affecting children, proliferative diabetic retinopathy (PDR), the wet form of age-related macular degeneration (AMD) and neovascular glaucoma affecting working-age and older adults, respectively (Penn et al., 2008). Small molecule antiangiogenic drugs are urgently needed to supplement the existing available biologics, including drugs such as bevacizumab, ranibizumab, and aflibercept, which target the vascular endothelial growth factzzor (VEGF) (Folk and Stone, 2010). Homoisoflavonoids, a class of compounds commonly found in the Scilloideae subfamily of the Asparagaceae family, have been shown previously to have potent anti-proliferative activities in endothelial cells over other cell types (Schwikkard et al., 2019). Moreover, they demonstrated a strong antiangiogenic potential in vitro and in vivo in animal models of ocular neovascularization (Sulaiman et al., 2016).

The genus *Rhodocodon* (Asparagaceae) has been the topic of much taxonomic debate and, in this work, we report on the phytochemical investigation into *Rhodocodon cryptopodus* (H. Perrier), *R. rotundus* (Baker) and *R. cyathiformis* (var. giganteus). The genus is endemic to Madagascar and thirteen species have been identified based on morphological, biogeographical and molecular evidence (Knirsch et al., 2015).

In the 1990s, Speta (Speta, 1998b) integrated the genus *Rhodocodon* into that of *Rhadamanthus*, effectively replacing the *Rhodocodon* genus, while *Rhadamanthus* was subsequently combined with *Drimia* by Manning et al., giving rise to the synonym *Drimia rotunda* (Manning et al., 2003). *Hyacinthus cryptopodus* (Baker) (syn. *Rhodocodon cryptopodus*), which had been placed in the Hyacinthoideae subfamily by Speta (Speta, 1998a) as the only Madagascan species in the *Hyacinthus* genus, was tentatively moved by Manning et al. (Manning et al., 2003) to the *Ledebouria* genus, pending further evidence, becoming *Ledebouria cryptopoda* (Baker) J. C. Manning and Goldblatt. This was due to characteristics unique to the *Ledebouria* genus such as the fibres produced when the bulb scales are torn. However, in 2006, this move was re-evaluated by Pfosser *et al.(Pfosser et al., 2006)*, who re-assigned *L. cryptopodus* to the subfamily Urgineoideae, which brought about a necessary transfer from the genus *Ledebouria* to *Drimia* as *D. cryptopoda* (Baker) Pfosser, Wetschnig & Speta. *Rhodocodon* Baker has recently been reinstated as a genus within the Scilloideae subfamily of the Asparagaceae (sensu APG III) by Knirsch *et al.*, (Knirsch et al., 2015) based on morphological, biogeographical and molecular evidence and *Drimia cryptopoda* was transferred to this new genus. No medicinal use of any species of *Rhodocodon* has been reported although the crushed bulbs of *R. cryptopodus* are used for epilation.

The aim of this work was to investigate the phytochemistry of the three *Rhodocodon* species and to evaluate the homoisoflavonoids isolated for their antiangiogenic activity.

Materials and methods

Instrumentation

NMR spectra were recorded on a 500 MHz Bruker AVANCE NMR spectrometer in either $CDCl_3$ or CD_3OD, UV-VIS spectra were recorded on a Libra Biochrom spectrometer in CH_3OH in a 1 cm cell, IR spectra were obtained using an Agilent (Cary 600 series) FTIR spectrometer (University of Surrey), ESIMS analysis was performed using an Alliance 2695 Quattro Ultra mass spectrometer, HRESIMS data were recorded on an Agilent 6550 iFunnel Q-TOF LC/MS with samples dissolved in CH_3OH. Optical rotations were measured at room temperature in CH_3OH

using a JASCO P-1020 polarimeter and CD spectra were measured on a Chirascan CD spectrometer using a 1 mm cell in CH_3CN. Solvents were reagent grade and purchased from Sigma-Aldrich.

Plant Material

Plant material of *Rhodocodon cryptopodus* (Baker), *Rhodocodon rotundus* (H. Perrier) and *R. cyathiformis* was collected by Dr Walter Knirsch in Madagascar. Collection permit: 215/13/MEF/SG/DGF/DCB.SAP/SCB, collected 27/12/2016 - 12/01/2017. Acquisition numbers of the collected plants are *R. cryptopodus*: 02442, *R. rotundus*: 04953 and *R. cyathiformis*: W[illegible]3. *R. cryptopodus* was collected from Ambatondradama, Madagascar, and purchased in the market of Antananarivo. *R. rotundus* was collected from along the roadside on the way to Sakalalina, Madagascar and *R. cyathiformis* was collected near Mahajanga at the Grotte d'Anjohibe. Voucher specimens have been retained at the Karl-Franzens-University, Graz, Austria.

Extraction and isolation

The dried bulbs of *R. cryptopodus* (67.5 g) were extracted with EtOH (550 mL) by shaking at room temperature for 24 hours. The EtOH extract (1.806 g) was obtained after solvent evaporation. The extract was separated using gravity column chromatography over silica gel (Merck 9385) to yield **1** (5.4 mg), **3** (3.5 mg), **6** (6.2 mg), **7** (2.9 mg), and **10** (3.7 mg). Dried bulbs of *R. rotundus* (269.2 g) were extracted at room temperature with continuous agitation over 24 hours with EtOH (200 mL). The resulting EtOH extract (18.1 g) was separated using a flash column chromatography system to yield compounds **2** (40.0 mg), **4** (7.8 mg), **5** (4.3 mg), **8** (40.7 mg) and **9** (11.4 mg). The fresh bulbs of *R. cyathiformis* (450 g) were extracted with CH_2Cl_2 (1 L) by shaking at room temperature for 42 hours. The extract (2.0 g) was separated using a flash column chromatography system (Biotage SP1 Flash Chromatography Purification System) to yield compounds **1** (1.0 mg) and **2** (1.1 mg). A detailed separation scheme of each extract can be found in the supporting information, along with spectra.

Compound characterisation

Compound **2** yellow oil; $[\alpha]_D^{23}$ +7.95 (*c* 0.86, MeOH); ECD (CH_3CN) λ (Δε) 230 nm (-0.2) 293 nm (+2.7), 310 nm (-0.1); ^1H NMR ($CDCl_3$, 500 MHz) and ^{13}C NMR ($CDCl_3$, 125 MHz) data are given in Table 1. HRESIMS *m/z* 315.0876 $[M-H]^-$ (calcd. for $[C_{17}H_{16}O_6 - H]$, *m/z* 315.0874).

Compound **9** white crystals; $[\alpha]_D^{23}$ +40.9 (*c* 0.44, MeOH); ^1H NMR ($CDCl_3$, 500 MHz) and ^{13}C NMR ($CDCl_3$, 125 MHz) data are given in Table 3. HRESIMS *m/z* 643.2728 $[M+Na]^+$ (calcd. for $[C_{32}H_{44}O_{12} + Na]$, *m/z* 643.2725).

Compound **10** white powder; ^1H NMR ($CDCl_3$, 500 MHz) and ^{13}C NMR ($CDCl_3$, 125 MHz) data are given in Table 2. ESIMS *m/z* 190.0631 $[M]^+$, (calcd. for $[C_{11}H_{10}O_3]^+$, *m/z* 190.0629).

Biological assay materials

Endothelial Growth Medium (EGM-2) was prepared by mixing the contents of an EGM-2 "Bullet Kit" (Cat. no. CC-4176) with Endothelial Basal Medium (EBM) (Lonza). The EGM-2 "Bullet Kit" contains hydrocortisone, human fibroblast growth factor (hFGF), VEGF, R3-insulin like growth factor (R3-IGF-1), ascorbic acid, human epidermal growth factor (hEGF), gentamycin and heparin along with 2% foetal bovine serum (FBS). Human Retinal Endothelial Cells (HRECs) and Attachment Factor were purchased from Cell Systems (Kirkland, WA, USA). HRECs used for cell proliferation studies were of varying passages (P6-P8) while cells used in tube formation assays were P4 and migration assays utilised P5. The complete medium used for culturing ARPE-19 cells (ATCC, Manassas, VA, USA) contained Ham's-F10 growth medium (Thermo Scientific, Waltham, MA, USA) + 10% FBS + 1% penicillin-streptomycin (pen–strep). 92-1 uveal melanoma cells (a kind gift of Dr. Martine Jager, University of Leiden) were grown in RPMI medium containing 10% FBS and 1% pen–strep. Y-79 retinoblastoma cells (a kind gift of Dr. Brenda L. Gallie, Ontario Cancer Institute) were grown in RB medium (IMDM + 10% FBS + 55 μM β-mercaptoethanol + 10 μg/mL insulin + 1% pen–strep). Matrigel was from Corning (Corning, NY, USA), while alamarBlue was from AbD Serotec (Raleigh, NC, USA).

Cell proliferation assays

Cells (2,500) in growth medium (100 µL) were incubated in the centre 48 wells of 96-well clear bottom black plates overnight, with the surrounding wells containing deionized, sterilised water (100 µL). This was followed by treatment of cells with 1 µL of different concentrations of each test compound. Compounds were tested in triplicate over the range of 1 mM to 1 nM (1% v/v final DMSO concentration). Treated cells were incubated for a further 44 hours. At the end of this incubation period, alamarBlue reagent (11.1 µL) was added and after 4 hours of incubation, fluorescence readings were taken with excitation and emission wavelengths of 560 nm and 590 nm respectively. Data were analysed and dose response curves generated using GraphPad Prism software (v. 7.0).

Migration assays

The scratch wound migration assay was performed as previously described (Basavarajappa et al., 2015) with HRECs grown in EGM-2 to confluency in a 12 well plate. A scratch was introduced with a sterile 10 µL pipette tip and medium was replaced with EGM-2 containing the indicated concentrations of compound with 1% DMSO/well and wells were imaged by brightfield microscopy to establish scratch width at t = 0. Cells that migrated into the scratch after 11 hours were manually counted and normalized to control. Statistical analysis using one-way ANOVA with Dunnett's *post hoc* tests to compare treatment with DMSO control was completed using GraphPad Prism. P-values < 0.05 were considered significant.

Tube formation assays

The Matrigel based tube formation assay was performed as previously described (Basavarajappa et al., 2015). Briefly, 50 µL Matrigel was allowed to solidify in a 96 well black, clear bottom plate at 37°C for 20 minutes. HRECs were added to the solid Matrigel at 15,000 cells/well in 100 µL EGM-2 and dosed with appropriate concentrations of compound with 1 µL DMSO/well. Tube formation was observed every 2 hours by brightfield microscopy and images were taken after 8 hours of tube formation. Six images per treatment were analysed with

AngiogenesisAnalyzer plugin for ImageJ (http://image.bio.methods.free.fr/ImageJ/?Angiogenesis-Analyzer-for-ImageJ), and total tubule length for treated cells was normalised to DMSO. Statistical analysis using one-way ANOVA with Dunnett's *post hoc* tests to compare treatment with DMSO control data was completed using GraphPad Prism.

Results

Isolation and characterization of compounds from R. cryptopodus

The EtOH extract of the bulbs of *R. cryptopodus* yielded a 3*S* 3-benzyl homoisoflavonoid, identified as 3*S*-(5,7-dihydroxy-(3'-hydroxy-4'-methoxybenzyl)-4-chromanone (**1**), previously reported from *Rhodocodon campanulatus* but not tested previously for angiogenic activity (Schwikkard et al., 2017), the cinnamic acid derivative, *p*-hydroxyphenylethyl *p*-coumarate (**3**), previously reported from *Dendrobium falconeri* (Orchidaceae), a species of orchid native to Asia, which showed a marginal inhibitory effect (EC_{50} of 352.1 µM) against Herpes simplex virus type 1 (HSV-1) (Sritularak and Likhitwitayawuid, 2009), two known bufadienolide glycosides, deglucohellebrin (**6**) and hellebrigenin (**7**), both of which have been isolated from the *Helleborous* genus (Ranunculaceae) (Watanabe et al., 2003) and the previously unreported coumarin (**10**). Compound **6** has been tested previously against oral human squamous carcinoma cells (HSC-2) and human melanoma cells (A 375) and was found to have a potent cytotoxic effect against both (GI_{50} = 2.8 nM and 6.3 nM respectively) (Watanabe et al., 2003). It was also found to have an inotropic effect on cat heart *in situ* and isolated guinea pig and rat hearts, while compound **7** is known to be cytotoxic against oral human squamous carcinoma cells (HSC-2) (GI_{50} = 2.9 nM) and human melanoma cells (A 375) (GI_{50} = 8.6 nM) (Watanabe et al., 2003). The structures of the compounds were determined using NMR spectroscopy and structures of known compounds were confirmed by comparison against literature values as referenced above. Complete NMR assignments for bufadienolides **6** – **9** (which are not available in the literature) are given (Table 3).

Compound **2**, 3*S*-5,7-dihydroxy-(4'-hydroxy-3'-methoxybenzyl)-4-chromanone, gave the same molecular formula ($C_{17}H_{16}O_6$), ESI-MS peak at *m/z* 315.0876 ($[M-H]^-$) and NMR spectrum (Table 1) as a homoisoflavonoid isolated previously from *Drimia delagoensis* (Koorbanally et al., 2005). However, an ECD study showed Cotton effects of +2.8 at 290 nm and −0.2 at 230 nm indicating the unusual 3*S* configuration (Moodley et al., 2006). This agrees with the reported configurations of other 3-benzyl homoisoflavonoids isolated from *Rhodocodon* which have also been found to have the 3*S* configuration (Schwikkard et al., 2017). Hence compound **2** is the *S*-enantiomer of the previously reported 3*R* isomer.

Compound **9**, 6α-acetoxy-3β,8β,14β-trihydroxy-10,13-dimethylbufa-4,20,22-trienolide 3-*O*-β-D-glucopyranoside, was found to be the 6α-acetoxy-analogue of scilliroside (6β-acetoxy-3β,8β,14β-trihydroxy-10,13-dimethylbufa-4,20,22-trienolide 3-*O*-β-D-glucopyranoside), a toxic compound from *Urginea maritima*, which has been used as a rodenticide (Bahri et al., 2000). ESI-MS analysis gave a $[M+Na]^+$ peak at *m/z* 643.2728, indicating a molecular formula of $C_{32}H_{44}O_{12}$ for the compound. Resonances attributable to carbons and protons of the bufadienolide lactone ring were present (Table 3) and correlations were seen between the H-17 resonance (δ_H 2.56, dd, *J*=9.2, 6.5 Hz) and the oxygenated C-14 resonance (δ_C 86.5) and the C-18 methyl carbon resonance (δ_C 15.8). The 3H-19 (δ_C 1.36) resonance showed correlations in the HMBC spectrum with the C-10 (δ_C 38.1), C-9 (δ_C 52.2) and alkene C-5 (δ_C 143.2) resonances. The C-10 resonance showed correlations with the H-4 alkene (δ_H 5.94, br s) and H-6 oxymethine resonances (δ_H 5.47, dd, *J*=8.6, 2.6 Hz). Coupling was seen in the COSY spectrum between the H-4 and H-3 (δ_H 4.26, bs) resonances. An acetate group was placed at C-6 due to a correlation seen between an acetate group carbonyl carbon resonance (δ_C 171.7) and the H-6 resonance. The orientation of H-6 was established as β as correlations were seen in the NOESY spectrum between the H-H-4/H-6, H-4/3H-19 and H-6/3H-19 resonances. The H-3 resonance showed a correlation with the acetate methyl group proton resonance. The specific rotation of compound **9** was found to be +40.9, while the literature value for scilliroside has been reported as -59.4 (Bahri et al., 2000).

LRMS of compound **10** indicated a molecular ion at *m/z*=190.2 corresponding to a molecular formula of $C_{11}H_{10}O_3$ and seven degrees of unsaturation. The NMR spectra indicated the presence of a substituted coumarin with the C-2 lactone carbonyl resonance occurring at δ_C 167.5

and the H-3 and H-4 resonances appearing as a pair of doublets at δ_H 5.64 and δ_H 7.41 (both d, *J*=7.8 Hz) respectively. The corresponding C-4 resonance (δ_C 143.7) showed a correlation with the H-5 resonance at δ_H 6.69 (d, *J*=8.0 Hz), which showed coupling in the COSY spectrum with the H-6 (δ_H 6.54, dd, *J*= 8.0, 2.1 Hz) and H-8 (δ_H 6.66, d, *J*=2.1 Hz) proton resonances. Both the H-6 and H-8 resonances showed correlations in the HMBC spectrum with the C-9 methylene carbon resonance (δ_C 39.9) and the corresponding 2H-9 triplet (δ_H 2.68, t, *J*=7.4 Hz) showed coupling with the 2H-10 oxymethylene proton resonance (δ_H 3.69, t, *J*=7.4 Hz), indicating a hydroxy group at C-10, in accordance with the molecular formula. Although 7-methylated and 7-prenylated coumarins and their derivatives are known, this is the first example of a 7-hydroxyethyl coumarin. It could possibly arise from the oxidative degradation of a prenyl group (El-Sharkawy and Mahmoud, 2016; Tantray et al., 2008; Tesso et al., 2005; Yang et al., 2013). Coumarins have not been reported previously from the Hyacinthaceae (Mulholland et al., 2013).

Isolation and characterization of compounds from R. rotundus and R. cyathiformis

The EtOH extract of the bulbs of *R. rotundus* yielded five compounds, two of which, a rare 3*S*-type 3-benzyl homoisoflavonoid (**2**) and a bufadienolide glycoside (**9**), have not been reported previously (Fig. 1). Two known cinnamic acid derivatives, *p*-hydroxyphenethyl-*trans*-ferulate (**4**), first extracted from *Heracleum lanatum* (Nakata et al., 1982) and 2-hydroxyethyl-*trans*-ferulate (ariscucurbin A) (**5**), previously isolated from *Aristolochia cucurbitifolia* (Wu et al., 1999), and 3β,14β-dihydroxy-19-oxo-5β-bufa-20,22-dienolide 3-O-β-D-glucopyranoside (**8**), reported once previously from the related Madagascan *Rhodocodon campanulatus* (Schwikkard et al., 2017) were isolated. Compound **4** is a known free-radical scavenger (Hirano et al., 1997) which has also been shown to have an affinity toward serotonin (5-HT_7) receptors (Kaewamatawong et al., 2007).

The CH_2Cl_2 extract of *R. cyathiformis* yielded compounds **1** and **2**, also isolated in this work from *R. cryptopodus* and *R. rotundus* respectively.

Antiproliferative effects of homoisoflavonoids

Homoisoflavonoids are known to inhibit angiogenesis with some selectivity for blocking the proliferation of endothelial cells over other ocular cell types (Basavarajappa et al., 2015; Lee et al., 2014). Thus, they have appeal as a basis for new treatments for neovascular eye diseases such as wet age-related macular degeneration (Sulaiman et al., 2014). Because of this, compounds **1** and **2** were tested for their anti-proliferative activities against human retinal endothelial cells (HRECs), giving excellent GI_{50} results of 0.13 µM and 0.49 µM respectively in this assay (Fig. 2). In comparison, the *R*-enantiomer of compound **1**, recently isolated from *Massonia bifolia* and tested for anti-proliferative activity against HRECs gave a GI_{50} of 93.2 µM (*R*), >700-fold less potent than *S*-enantiomer **1** (Schwikkard et al., 2018).

Although compounds **1** and **2** are very similar in structure and gave similar GI_{50} results against the endothelial cell line, HRECs, the compounds showed very different activities against other cell lines. Compounds were tested for their specificity against human retinal pigmented epithelial cells (ARPE-19) as well as retinoblastoma (Y-79) and uveal melanoma (92-1) cell lines (Fig. 2). Compound 1 was found to be non-specific, with GI_{50} values ranging from 0.21 – 0.85 µM across the four cell types, while compound **2** showed at least 100-fold specificity for HRECs over the other tested cell lines (Fig. 2).

Antiangiogenic effects of homoisoflavonoids

Both compounds **1** and **2** were tested for inhibition of key *in vitro* angiogenic properties of HRECs, migration and tubule formation, and showed dose-dependent blockade of both these properties (Figs. 3 and 4).

Discussion

The limitations of existing therapies for neovascular eye diseases like wet age-related macular degeneration provide a compelling need for novel pharmacological approaches. There is a growing body of evidence showing that homoisoflavonoids have antiangiogenic activity relevant to

these diseases, in some cases with limited effects on non-target cells. Thus, in this study we sought novel homoisoflavonoids from a plant genus known to produce this class of compounds, and tested isolated compounds for antiangiogenic activity.

Despite the similarity in structure of compounds **1** and **2**, compound **1** was non-specific for antiproliferative effects on endothelial cells, while compound **2** was selective for HRECs. However, both compounds blocked migration and tubule formation of HRECs; these assays provide a good in vitro model of antiangiogenic activity. Taken together, these results suggest that compound **2** shows promise for the development of future small molecule treatments for ocular neovascularization, due to its specificity and its excellent activity against HRECs.

Conflicts of interest

There are no conflicts to declare.

Acknowledgements

H. Whitmore acknowledges a PhD scholarship from the University of Surrey. Sianne Schwikkard acknowledges support from the Daphne Jackson Trust, the University of Surrey and the Royal Society of Chemistry for funding. T. W. Corson acknowledges support from NIH/NEI R01EY025641, the BrightFocus Foundation, and an unrestricted grant from Research to Prevent Blindness, Inc.

References

Bahri, L., Djegham, M., Makhlouf, M., 2000. *Urginea maritima* A poisonous plant of North Africa. Vet. Hum. Toxicol. 42, 108-110.

Basavarajappa, H., Lee, B., Lee, H., Sulaiman, H., An, H., Magaña, C., Shadmand, M., Vayl, A., Rajashekhar, G., Kim, E., Suh, Y., Lee, K., Seo, S., Corson, T., 2015. Synthesis and Biological Evaluation of Novel Homoisoflavonoids for Retinal Neovascularization. J. Med. Chem. 58, 5015-5057.

El-Sharkawy, E.R., Mahmoud, K., 2016. Cytotoxity of two new coumarin derivatives isolated from *Launaea mucronata*. Nat. Prod. Res. 30, 394-398.

Folk, J.C., Stone, E.M., 2010. Ranibizumab Therapy for Neovascular Age-Related Macular Degeneration. N. Engl. J. Med. 363, 1648-1655.
Hirano, H., Tokuhira, T., Yokoi, T., Shingu, T., 1997. Isolation of free radical scavenger from *Coptidis rhizoma*. J. Nat. Med. 51, 539-540.
Kaewamatawong, R., Ruangrungsi, N., Likhitwitayawuid, K., 2007. Chemical constituents of *Polyalthia parviflora* stem. J. Nat. Med. 61, 349–350.
Knirsch, W., Martínez-Azorín, M., Pfosser, M., Wetschnig, W., 2015. The reinstatement and rediagnosis of the Madagascan genus *Rhodocodon* (Asparagaceae, Scilloideae), with validation and remarks on H. Perrier's taxa. Phytotaxa 195, 101–134.
Koorbanally, C., Mulholland, D., Crouch, N., 2005. A novel homoisoflavonoid from *Drimia delagoensis* (Urgineoideae: Hyacinthaceae). Biochem. Syst. Ecol. 33, 743-748.
Lee, B., Basavarajappa, H., Sulaiman, R., Fei, X., Seo, S., Corson, T., 2014. The first synthesis of the antiangiogenic homoisoflavone, cremastranone. Org. Biomol. Chem. 12, 7673-7677.
Manning, J.C., Goldblatt, P., Fay, M., 2003. Revised generic synopsis of Hyacinthaceae in sub-Saharan Africa, based on molecular evidence, including new combinations and the new tribe Pseudoprospereae. Edinb. J. Bot. 60, 533-568.
Moodley, N., Crouch, N., Mulholland, D., Slade, D., Ferreira, D., 2006. 3-Benzyl-4-chromanones (homoisoflavanones) from bulbs of the ethnomedicinal geophyte *Ledebouria revoluta* (Hyacinthaceae). S. Afr. J. Bot. 72, 517-520.
Mulholland, D.A., Schwikkard, S.L., Crouch, N.R., 2013. The chemistry and biological activity of the Hyacinthaceae. Nat. Prod. Rep. 30, 1165-1210.
Nakata, H., Sashida, Y., Shimomura, H., 1982. A new phenolic compound from *Heracleum lanatum* MICHX. var. *nippinicum* HARA. II. Chem. Pharm. Bull. 30, 4554-4556.
Penn, J.S., Madan, A., Caldwell, R.B., Bartoli, M., Caldwell, R.W., Hartnett, M.E., 2008. Vascular endothelial growth factor in eye disease. Prog. Retin. Eye Res. 27, 331-371.
Pfosser, M., Wetschnig, W., Speta, F., 2006. *Drimia cryptopoda*, a new combination in Hyacinthaceae from Madagascar. Linz. Biol. Beitr. 38, 1731-1739.
Schwikkard, S., Alqahtani, A., Knirsch, W., Wetschnig, W., Jaksevicius, A., Opara, E., Langat, M., Andriantiana, J., Mulholland, D., 2017. Phytochemical Investigations of Three R*hodocodon* (Hyacinthaceae Sensu APG II) Species. J. Nat. Prod. 80, 30-37.
Schwikkard, S., Whitmore, H., Sishtla, K., Sulaiman, R.S., Shetty, T., Basavarajappa, H.D., Waller, C., Alqahtani, A., Frankemoelle, L., Chapman, A., Crouch, N., Wetschnig, W., Knirsch, W., Andriantiana, J., Mas-Claret, E., Langat, M.K., Mulholland, D., Corson, T.W., 2019. The Antiangiogenic Activity of Naturally Occurring and Synthetic Homoisoflavonoids from the Hyacinthaceae (*sensu* APGII). J. Nat. Prod. 82, 1227-1239.
Schwikkard, S.L., Whitmore, H., Corson, T.W., Sishtla, K., Langat, M.K., Carew, M., Mulholland, D.A., 2018. Antiangiogenic Activity and Cytotoxicity of Triterpenoids and Homoisoflavonoids from *Massonia pustulata* and *Massonia bifolia*. Planta Med. 84.

Speta, F., 1998a. The Families and Genera of Vascular Plants III. Flowering Plants, Monocotyledons: Lilianae (Except Orchidaceae), in: Kubitzki, K. (Ed.). Springer, Berlin, pp. 261-285.

Speta, F., 1998b. Systematische Analyse der Gattung *Scilla* L. s. l. (Hyacinthaceae). Phyton 38, 1-141.

Sritularak, B., Likhitwitayawuid, K., 2009. New Bisbibenzyls from *Dendrobium falconeri*. Helv. Chim. Acta 92, 740-744.

Sulaiman, R., Basavarajappa, H., Corson, T., 2014. Natural product inhibitors of ocular angiogenesis. Exp. Eye Res. 129, 161-171.

Sulaiman, R.S., Merrigan, S., Quigley, J., Qi, X., Lee, B., Boulton, M.E., Kennedy, B., Seo, S.Y., Corson, T.W., 2016. A novel small molecule ameliorates ocular neovascularisation and synergises with anti-VEGF therapy. Sci. Rep. 6, 25509.

Tantray, M.A., Bhat, B.A., Khuroo, M.A., Shawl, A.S., 2008. Two new coumarins from *Euonymus hamiltonianus*. Chem. Nat. Compd. 44, 10-12.

Tesso, H., König, W.A., Kubeczka, K.-H., Bartnik, M., Glowniak, K., 2005. Secondary metabolites of *Peucedanum tauricum* fruits. Phytochemistry 66, 707-713.

Watanabe, K., Mimaki, Y., Sakagami, H., Sashida , Y., 2003. Bufadienolide and spirostanol glycosides from the rhizomes of *Helleborus orientalis*. J. Nat. Prod. 66, 236-241.

Wu, T., Leu, Y., Chan, Y., 1999. Constituents of the Fresh Leaves of *Aristolochia cucurbitifolia*. Chem. Pharm. Bull. 47, 571-573.

Yang, X.-L., Awakawa, T., Wakimoto, T., Abe, I., 2013. Induced production of novel prenyldepside and coumarins in endophytic fungi *Pestalotiopsis acaciae*. Tetrahedron Lett. 54, 5814-5817.

Table Legends.

Table 1. NMR data for compounds **1** and **2** (500 MHz, $CDCl_3$, *J* in Hz).

Table 2. NMR Data for Compound **10** (500 MHz, $CDCl_3$, *J* in Hz).

Table 3. NMR Data for Compounds **6-9** (500 MHz, $CDCl_3$, *J* in Hz).

Table 4. NMR data for compounds **1** and **2** (500 MHz, $CDCl_3$, *J* in Hz)

	1		**2**	
No.	δ_C	δ_H	δ_C	δ_H
2	69.3	(α) 4.11 (dd, 11.4, 7.4)	69.1	(α) 4.10 (dd, 11.5,7.0)
		(β) 4.27 (dd, 11.4, 4.3)		(β) 4.26 (dd, 11.5,4.2)
3	46.9	2.83 (m)	46.8	2.80 (m)
4	198.1	-	198.3	-
4a	103.0	-	102.6	-
5	164.9	-	165.3	-
6	96.8	5.98 (d, 2.2)	96.9	6.01 (d, 2.5)
7	164.4	-	164.7	-
8	95.2	5.91 (d, 2.2)	95.4	5.93 (d, 2.5)
8a	163.5	-	163.4	-
9	32.4	(a) 3.16 (dd, 14.0, 4.6)	32.4	(a) 3.14 (dd, 13.9,4.5)
		(b) 2.65 (dd, 14.0, 10.6)		(b) 2.63 (dd, 13.9,7.0)
1’	131.1	-	131.2	-
2’	115.4	6.81 (d, 1.9)	115.4	6.80 (d, 2.3)
3’	146.0	-	145.8	-
4’	145.7	-	145.7	-
5’	111.0	6.80 (d, 8.1)	111.1	6.79 (d, 8.2)
6’	120.8	6.70 (dd, 8.1, 1.9)	120.9	6.70 (dd, 8.2,2.3)
3’-OMe	-	-	56.2	3.88 (s)
4’-OMe	56.2	3.88 (s)	-	-
5-OH	-	12.13 (s)	-	12.15 (s)

Table 5. NMR Data for Compound **10** (500 MHz, $CDCl_3$, *J* in Hz).

10						
No.	^{13}C	Type	^{1}H (*J* in Hz)	HMBC (H→C)	COSY	NOESY
2	167.5	C				
3	101.9	CH	5.64 (d, 7.8)	4	4	4
4	143.7	CH	7.41 (d, 7.8)	2, 3, 4a	3	3
4a	144.8	C				
5	116.4	CH	6.69 (d, 8.0)	4, 4a, 6, 7	6	6
6	121.3	CH	6.54 (dd, 8.0 2.1)	4a, 5, 8	5	5, 9
7	131.9	C				
8	117.3	CH	6.66 (d, 2.1)	4a, 6		6, 9
8a	151.7	C				
9	39.9	CH_2	2.68 (t, 7.4)	6, 7, 8, 10	10	6, 8, 10
10	64.8	CH_2	3.69 (t, 7.4)	7, 9	9	9

Table 6. NMR Data for Compounds **6-9** (500 MHz, $CDCl_3$, *J* in Hz).

	6		**7**		**8**		**9**		
No.	δ_C	δ_H	δ_C	δ_H	δ_C	δ_H	δ_C	δ_H	HMBC (H → C)
1	23.7	(α) 1.57 (d, 2.5)	23.7	(α) 1.54 br s	32.8	(α) 2.03 (m)*	39.2	(α) 1.87 (m)	3, 5, 9, 10
		(β) 1.18 (s)		(β) 1.17 (d, 2.1)		(β) 1.69 (m)		(β) 1.38 (d)*	
2	29.8	(α) 2.23 (m)	29.8	(α) 2.22 (d, 3.5)	28.8	(α) 2.27 (dd, 12.8, 2.7)	27.7	(α) 2.08 (m)	
		(β) 1.77 (t, 3.7)		(β) 1.77 (d, 1.92)		(β) 1.32 (d, 5.0)*		(β) 1.77 (m)	
3	75.1	4.17 (bs, $W_{1/2}$ = 8.4 Hz)	74.9	4.26 (bs, $W_{1/2}$ = 9.1 Hz)	78.6	3.78 (m, $W_{1/2}$ = 24.5 Hz)	77.0	4.29 (bt, $W_{1/2}$ = 20.7)	4, 5, 1'
4	37.4	(α) 2.17 (d, 4.3)	35.6	(α) 2.17 s	36.9	(α) 1.95 (m)	131.7	5.94 (br s)	2, 6, 10
		(β) 1.71 (d, 4.7)		(β) 1.76 (d, 3.7)		(β) 1.31 (d, 5.0)*			-
5	75.3	-	75.0	-	44.3	1.63 (m)	143.2	-	4, 5, 8, 10, 6-OAc(a)
6	36.4	(α) 2.22 (d, 4.9)	38.0	(α) 2.14 (d, 2.8)	32.3	(α) 2.43 (dt, 13.6, 3.2)	77.6	5.47 (dd, 8.6, 2.6)	5, 6, 8, 9, 14
		(β) 1.64 (t, 2.8)		(β) 1.71 (d, 5.0)		(β) 1.05 (td, 14.0, 3.5)			
7	19.2	(α) 2.09 (m)	19.1	(α) 2.18 (d, 3.0)	30.3	(α) 2.58 (s)	38.7	(α) 2.39 (dd, 15.5, 2.3)	-
		(β) 1.78 (m)		(β) 1.71 (d, 4.9)		(β) 2.02 (m)*		(β) 1.69 (m)	10, 19

8	40.7	1.74 (d, 3.3)	40.7	1.73 m	44.1	1.42 (m)	77.5	-	-
9	43.2	1.98 (d, 2.8)	43.1	1.98 (d, 2.9)	49.9	1.30 (m)	52.2	1.43 (m)	9, 10
10	56.3	-	56.4	-	53.0	-	38.1	-	8, 13
11	25.4	(α) 2.21 (br s)	25.5	(α) 2.20 (d, 1.77)	23.3	(α) 1.74 (dd, 13.0, 5.0)	19.4	(α) 1.86 (m)	9, 11, 13, 14
		(β) 1.42 (d, 3.8)		(β) 1.40 m		(β) 1.21 (d, 7.1)		(β) 1.49 (m)	13
12	41.6	(α) 1.52 (d, 3.2)	41.6	(α) 1.52 (d, 2.0)	41.5	(α) 1.51 (t, 3.1)	42.1	(α) 1.45 (m)	-
		(β) 1.47 (d, 4.1)		(β) 1.44 br s		(β) 1.40 (d, 3.0)		(β) 1.62 (m)	-
13	49.0	-	49.0	-	49.6	-	50.5	-	8, 16
14	85.8	-	85.8	-	85.6	-	86.[illegible]	-	14, 16, 17
15	32.5	(α) 2.12 (d, 2.9)	32.5	(α) 2.10 (d, 5.0)	31.7	(α) 2.01 (m)*	35.1	(α) 2.05 (d)*	13, 14, 15, 20
		(β) 1.69 (d, 5.7)		(β) 1.70 (d, 3.7)		(β) 1.34 (m)		(β) 1.68 (d, 8.4)	13, 14, 17, 20
16	26.2	(α) 1.86 (m)	26.3	(α) 1.90 m	29.8	(α) 2.19 (dt, 12.6, 9.8)	30.2	(α) 2.19 (m)	12, 13, 14, 16, 20, 22
		(β) 1.72 (d, 4.9)		(β) 1.69 (d, 4.0)		(β) 1.62 (d, 9.[illegible])		(β) 1.72 (m)	12, 13, 14, 17
17	52.1	2.58 (dd, 9.4, 6.5)	52.1	2.57 (dd, 9.6, 6.7)	52.2	2.55 (dd, 9.4, 6.[illegible])	52.9	2.56 (dd, 9.2, 6.5)	1, 5, 9, 10
18	17.2	0.70 (s)	17.2	0.70 s	17.2	0.67 (s)	19.8	0.92 (s)	-
19	209.8	10.10 (s)	210.2	10.08 s	210.7	10.01 (s)	22.4	1.36 (s)	17, 20, 22, 24
20	125.0	-	125.0	-	125.0	-	125.3	-	17, 21, 24
21	150.7	7.45 (dd, 2.4, 0.8)	150.7	7.44 (d, 1.7)	150.6	7.44 (d, 1.7)	150.6	7.43 (d, 1.6)	20, 24
22	149.4	8.01 (dd, 9.7, 2.4)	149.4	8.00 (dd, 12.3, 2.0)	149.4	7.99 (dd, 9.7, 2.4)	149.4	8.03 (dd, 9.7, 2.5)	-
23	115.6	6.30 (dd, 9.7, 0.6)	115.6	6.30 (d, 9.7)	115.6	6.30 (d, 9.7)	115.6	6.31 (d, 9.7)	3, 3’
24	164.9	-	164.9	-	164.9	-	165.0	-	1’, 4’
1’	101.1	4.87 m*	102.0	4.43 (d, 7.9)	102.5	4.40 (d, 7.8)	103.8	4.43 (d, 7.7)	1’, 2’, 4’, 5’
2’	72.6	3.63 (d, 3.3)	75.2	3.19 (dd, 9.2, 7.9)	75.2	3.14 (dd, 9.0, 7.8)	75.2	3.19 (dd, 9.2, 7.7)	3’, 5’
3’	72.7	3.80 (dd, 3.2, 1.8)	78.4	3.37 m	78.1	3.37 (m)	78.2	3.38 (t, 8.8)	4’, 6’
4’	73.9	3.42 (t, 9.4)	78.3	3.29* m	78.0	3.28 (d, 1.5)	78.1	3.29 (br s)	4’, 5’
5’	70.8	3.65 m	71.8	3.30* m	71.8	3.29 * m	71.8	3.31 (d, 7.6)	4’, 5’
6’	18.1	1.29 (d, 6.2)*	62.9	(a) 3.98 (d, 11.6)	62.9	(a) 3.88 (d, 11.4)	62.9	(a) 3.88 (m)	
				(b) 3.70 (dd, 11.6, 5.1)		(b) 3.67 (m)		(b) 3.68 (dd, 11.7, 5.2)	
6-OAc	-	-	-	-			171.7	-	
	-	-		-			21.7	2.04 (s)*	

*=overlapped resonances.

Figure Legends.

Fig. 1. Compounds isolated from *R. cryptopodus, R. rotundus* and *R. cyathiformis*.

Fig. 2. Dose-response curves for inhibition of proliferation of indicated cell types by compounds **1** and **2**. Mean±SEM, n=3.

Fig. 3. Migration assays for HRECs treated with compounds **1** and **2**. Representative images of the highest concentration treatment of each compound or DMSO control shown (scale bars = 1 mm) and quantification of migrated cells. Mean±SEM, n=3. ***, $P < 0.001$ compared to DMSO, ANOVA with Dunnett's *post hoc* tests.

Fig. 4. Tube formation assays for HRECs treated with compounds **1** and **2**. Representative images of highest concentration treatment of each compound or DMSO control shown (scale bars = 1 mm) along with quantification of tubule length, Mean±SEM, n=6. **, $P < 0.01$; ***, $P < 0.001$, ANOVA with Dunnett's *post hoc* tests.

Figures and tables

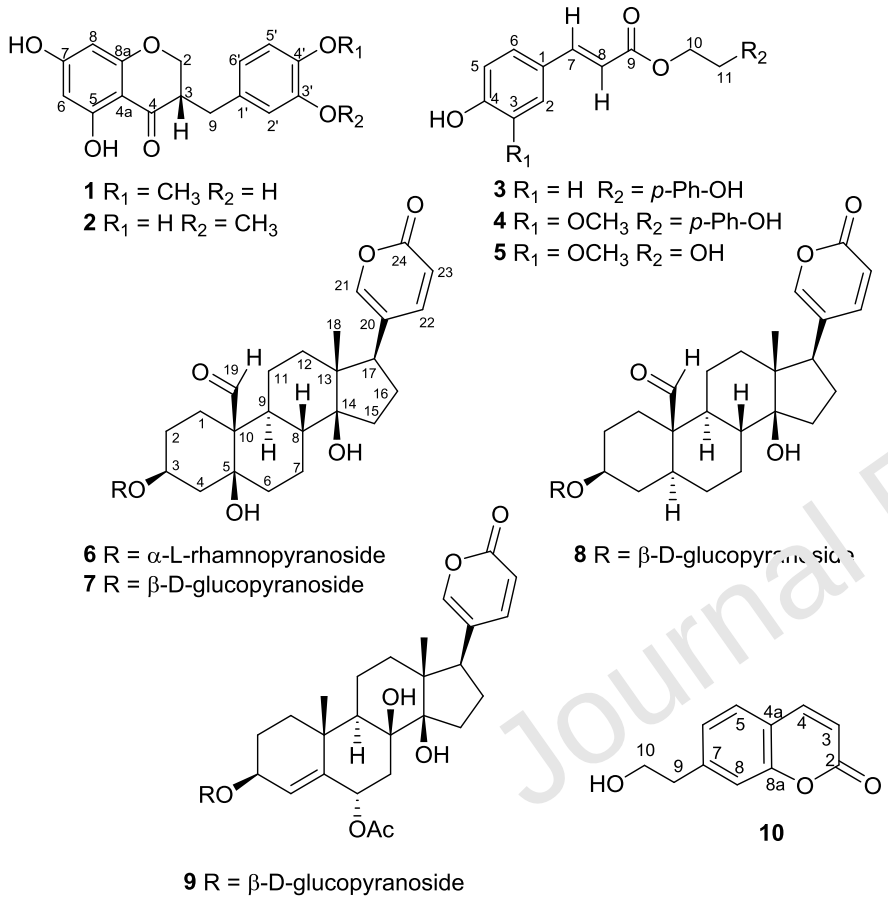

Fig. 5. Compounds isolated from *R. cryptopodus*, *R. rotundus* and *R. cyathiformis*.

Compound	HREC GI_{50} (μM)	ARPE-19 GI_{50} (μM)	92-1 GI_{50} (μM)	Y79 GI_{50} (μM)
1	0.13	0.85	0.21	0.83
2	0.49	40	28	>100

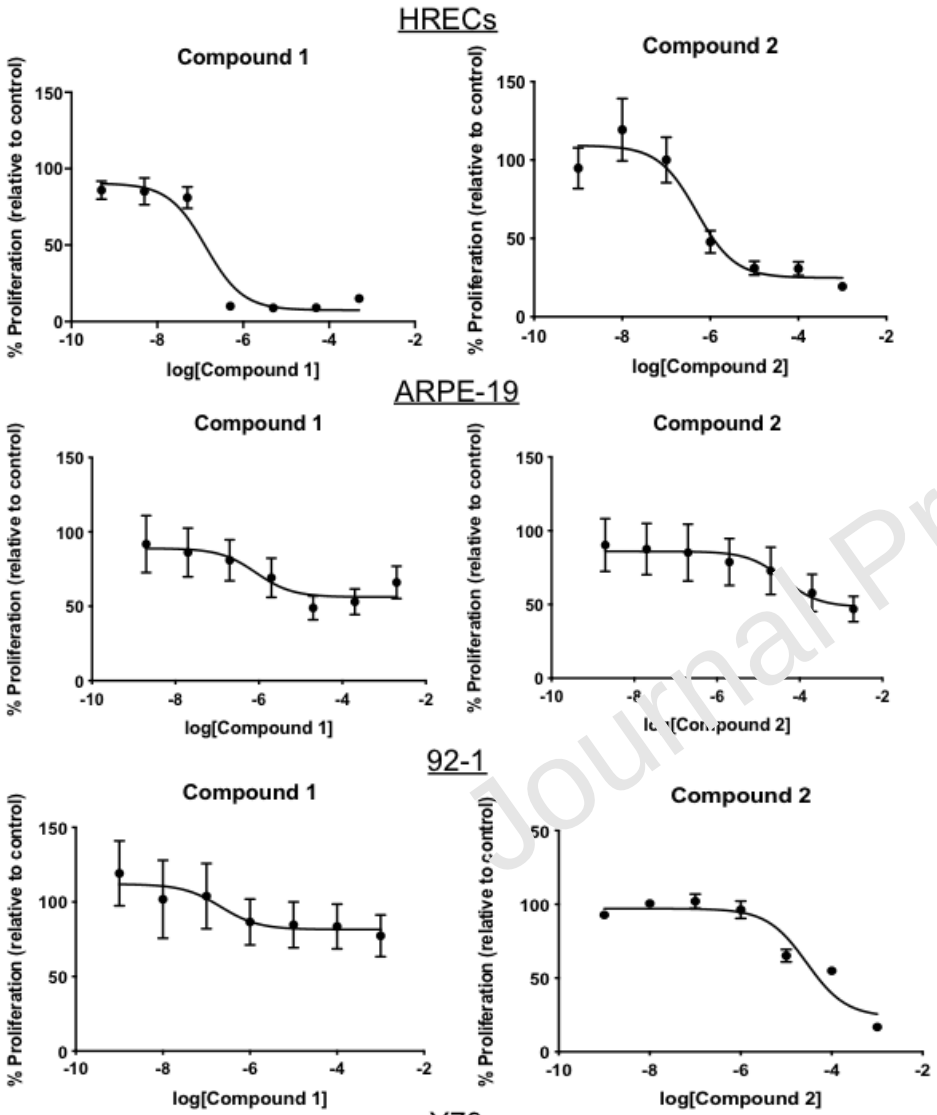

Fig. 6. Dose-response curves for inhibition of proliferation of indicated cell types by compounds **1** and **2**. Mean±SEM, n=3.

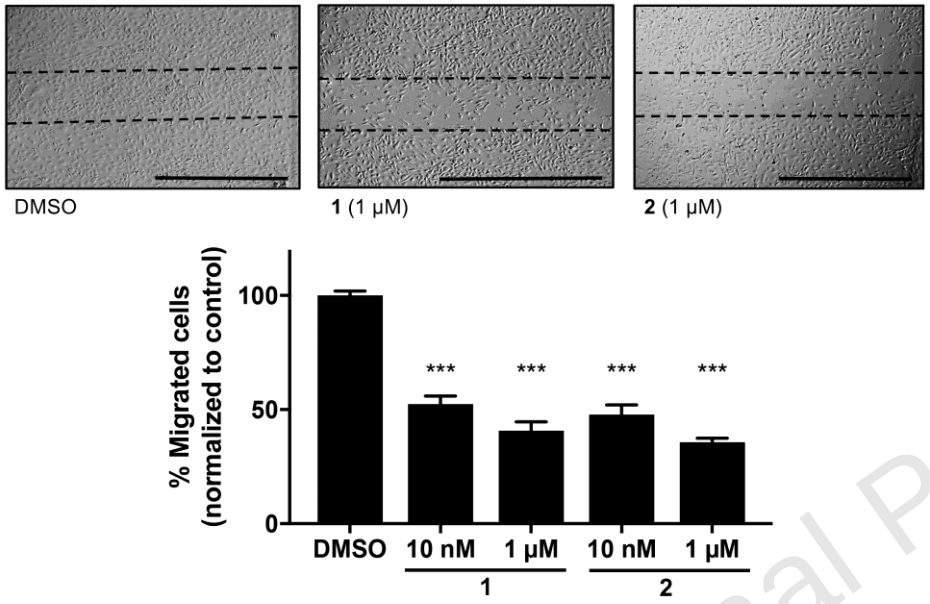

Fig. 7. Migration assays for HRECs treated with compounds **1** and **2**. Representative images of the highest concentration treatment of each compound or DMSO control shown (scale bars = 1 mm) and quantification of migrated cells. Mean±SEM, n=3. ***, $P < 0.001$ compared to DMSO, ANOVA with Dunnett's *post hoc* tests.

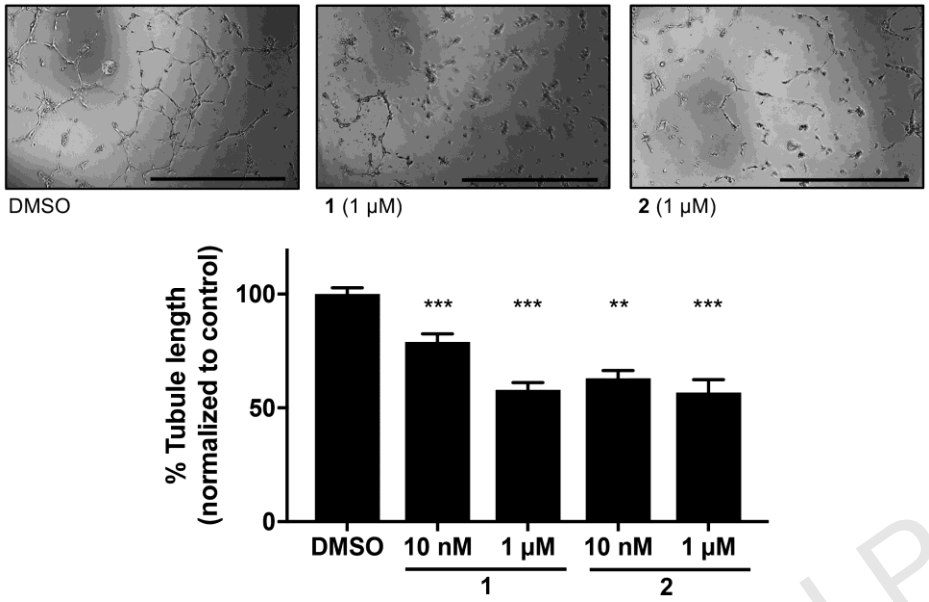

Fig. 8. Tube formation assays for HRECs treated with compounds **1** and **2**. Representative images of highest concentration treatment of each compound or DMSO control shown (scale bars = 1 mm) along with quantification of tubule length, Mean±SEM, n=6. **, P < 0.01; ***, P < 0.001, ANOVA with Dunnett's *post hoc* tests.